

# Tau physics at the LHC with ATLAS

Stan Lai  
on behalf of the ATLAS Collaboration

*Albert-Ludwigs Universität Freiburg, 79104, Freiburg, Germany*

**Abstract.** The presence of  $\tau$  leptons in the final state is an important signature in searches for physics beyond the Standard Model. Hadronically decaying  $\tau$  leptons can be reconstructed over a wide kinematic range at ATLAS. The reconstruction algorithm for hadronically decaying  $\tau$  leptons and the performance of  $\tau$  lepton identification is described. A review of physics processes with  $\tau$  lepton final states is given, ranging from Standard Model processes in early data, such as  $W$  and  $Z$  boson production, to searches for new phenomena beyond the Standard Model.

**Keywords:** Tau lepton, ATLAS

**PACS:** 14.60.Fg

## Introduction

The  $\tau$  lepton, with a mass of  $m_\tau = 1776.84 \pm 0.17$  MeV [1], is the only lepton heavy enough to decay both leptonically and hadronically. It decays approximately 65% of the time to one or more hadrons and 35% of the time leptonically. The reconstruction and identification of  $\tau$  leptons are important in many searches for new phenomena, and they can appear in final states in the production of Higgs bosons, supersymmetric (SUSY) particles, and other particles not described by the Standard Model [2, 3]. Standard Model processes, such as the  $W$ ,  $Z$  boson and  $t\bar{t}$  production can also result in signatures with  $\tau$  leptons, and events from these processes can be used to measure key quantities such as the  $\tau$  lepton identification efficiency for the ATLAS reconstruction algorithm.

A challenge in identifying hadronically decaying  $\tau$  leptons ( $\tau_{\text{had}}$ ) is to distinguish them from hadronic jets which are produced in processes with very large cross-sections. However,  $\tau_{\text{had}}$  leptons possess certain properties that can be used to differentiate them from jets. They usually decay into one (1-prong) or three (3-prong) charged particles and their decay products are well collimated with an invariant mass less than  $m_\tau$ . The  $\tau$  lepton proper lifetime is  $87 \mu\text{m}$ , leading to decay vertices that can be resolved in the silicon tracker from the primary interaction vertex. In addition,  $\tau_{\text{had}}$  leptons deposit a considerable fraction of their visible energy in the electromagnetic calorimeter in contrast with jets which deposit their energy primarily in the hadronic calorimeter.

## The reconstruction and identification of $\tau$ leptons

Hadronically decaying  $\tau$  candidates are reconstructed at ATLAS using two seed types. The first seed type is a track with  $p_T > 6$  GeV that satisfies quality criteria on the number of associated silicon hits and the impact parameter with respect to

the interaction vertex. The second type of seed consists of jets reconstructed using topological clusters (topoclusters) [2] with  $E_T > 10$  GeV. Topoclusters are formed using cells that exceed calorimeter noise by  $4\sigma$ . Neighbouring cells that exceed energy thresholds above calorimeter noise by  $2\sigma$  and  $0\sigma$  are associated to the cluster in a second and third step, respectively. These topoclusters are then grouped into a topojet using a seeded cone algorithm [4] with a cone radius of  $\Delta R = 0.4$  which forms seeds for  $\tau_{\text{had}}$  candidates. These topojets are then matched to the seed tracks in a cone of radius  $\Delta R = 0.2$  around the topojet. If such a match is found, the  $\tau_{\text{had}}$  candidate is considered as having two valid seeds. For reconstructed  $\tau_{\text{had}}$  leptons in  $Z \rightarrow \tau\tau$  events with  $p_T > 10$  GeV and  $|\eta| < 2.5$ , 70% of  $\tau_{\text{had}}$  candidates have two valid seeds, 25% have only a topojet seed, and 5% have only a track seed.

The energy of the  $\tau_{\text{had}}$  candidate is calculated in two ways. For  $\tau_{\text{had}}$  candidates with a topojet seed, the cells in a cone of  $\Delta R = 0.4$  are summed and weighted according to a function dependent on the  $\eta$ ,  $\phi$  and calorimeter layer of the cell, similar to the method used for the Liquid Argon calorimeter of the H1 experiment [5]. For  $\tau_{\text{had}}$  candidates with a track seed, an energy flow approach is used, where energy deposits in cells matched to charged tracks are subtracted and replaced by the momenta of such tracks. This energy of the  $\tau_{\text{had}}$  candidate is also corrected for energy leakage coming from charged particles outside the narrow cone.

Tracks associated to the  $\tau_{\text{had}}$  candidate in a cone of  $\Delta R = 0.2$  are also required to pass track quality criteria on the number of associated hits in the silicon tracker and the impact parameter to the interaction vertex. Topoclusters found in the electromagnetic (EM) calorimeter with  $E_T > 1$  GeV that are isolated from tracks are interpreted as energy deposits from  $\pi^0$  mesons in the  $\tau$  lepton decay. This procedure finds that approximately 66% of  $\tau \rightarrow \pi\nu$  decays are reconstructed with zero  $\pi^0$  subclusters, while more than 50% of  $\tau \rightarrow \rho\nu$  ( $\tau \rightarrow a_1\nu$ ) decays are reconstructed with one (two)  $\pi^0$  subcluster(s).

Based on the calorimeter information, the associated tracks and reconstructed  $\pi^0$  clusters, a variety of other variables are calculated to be used for the identification of  $\tau_{\text{had}}$  leptons. These variables include the radius of energy deposits of the  $\tau_{\text{had}}$  candidate in the EM calorimeter (shown in Fig. 1 [left]), isolation variables for the calorimeter energy and tracks, the reconstructed charge (based on the associated tracks), the invariant mass of the  $\tau_{\text{had}}$  candidate (with and without  $\pi^0$  subclusters), the impact parameter significance of the leading track, ratios of energy deposits to the sum of track transverse momenta, and the transverse flight path significance of the  $\tau_{\text{had}}$  candidate vertex (for  $\tau_{\text{had}}$  candidates with more than one track).

Muons are vetoed by requiring that the calorimetric energy deposited by the  $\tau_{\text{had}}$  candidate has  $E_T > 5$  GeV. For electrons, cuts are placed upon  $\tau_{\text{had}}$  candidates on the following two quantities: the ratio of the transverse energy deposited in the EM calorimeter to the track transverse momentum which tends to be higher for electrons than for charged hadrons; and the ratio of high threshold hits to low threshold hits in the Transition Radiation Tracker for the track, which also tends to be higher for electrons. This veto suppresses electrons by a factor of 60, while retaining 95% of  $\tau_{\text{had}}$  leptons.

Many identification methods that use the reconstructed variables to suppress fake  $\tau_{\text{had}}$  lepton candidates from hadronic jets are studied at ATLAS, including cut-based identification, a projective likelihood, neural networks, and boosted decision trees. The rejection against jets as a function of identification efficiency for  $\tau_{\text{had}}$  leptons is shown

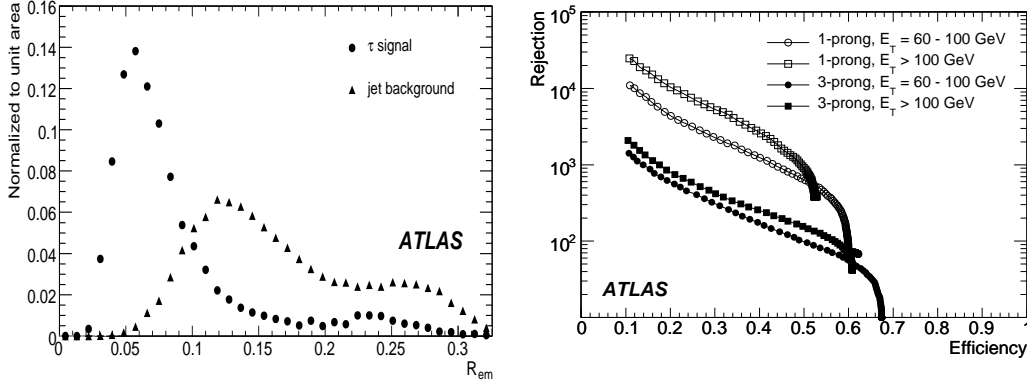


**FIGURE 1.** Left: The distribution of the reconstructed radius in the EM calorimeter ( $R_{EM}$ ) for  $\tau_{\text{had}}$  leptons and hadronic jets. Right: Rejection against jets as a function of  $\tau$  lepton efficiency for the projective likelihood identification method for 1-prong and 3-prong candidates with  $p_T^{\tau} = 60 - 100$  and  $> 100$  GeV.

in Fig. 1 (right) for the projective likelihood for 1-prong and 3-prong candidates.

## Standard Model processes with $\tau$ final states

The process  $W \rightarrow \tau\nu$  has a cross-section of  $1.7 \times 10^4$  pb at  $E_{CM} = 14$  TeV and it will be the most abundant source of  $\tau$  leptons at ATLAS. Events from this process will be selected by a  $\tau_{\text{had}}$  lepton +  $E_T^{\text{miss}}$  trigger, which has an efficiency of 70% with respect to offline selection, and can only be run during luminosities less than  $10^{32} \text{cm}^{-2} \text{s}^{-1}$ . Events are selected by requiring a  $\tau_{\text{had}}$  lepton with  $20 < p_T < 60$  GeV, an additional jet with  $p_T > 15$  GeV, and  $E_T^{\text{miss}} > 60$  GeV not pointing in the direction of the jet or  $\tau_{\text{had}}$  lepton candidate. Events that have an isolated electron or muon are also vetoed.

The dominant background to this process is QCD dijet production, which has a production cross-section that is approximately six orders of magnitude greater than that for  $W \rightarrow \tau\nu$ . Other backgrounds that contribute include  $W \rightarrow e\nu$ ,  $W \rightarrow \mu\nu$ ,  $t\bar{t}$ ,  $Z \rightarrow \tau\tau$ , and  $Z \rightarrow ee$ . The signal to background ratio is very sensitive to the cut on  $E_T^{\text{miss}}$ . A cut of  $E_T^{\text{miss}} > 50$  GeV leads to a signal to background ratio of 1:1, while increasing this threshold to 60 GeV yields 3:1 for this ratio with 1550 signal events expected in  $100 \text{pb}^{-1}$  of integrated luminosity. Therefore the scale and systematic effects of  $E_T^{\text{miss}}$  will have to be well under control. Fig. 2 shows the track multiplicity spectrum for  $\tau$  candidates in signal and background processes for  $100 \text{pb}^{-1}$  of integrated luminosity.

The  $Z \rightarrow \tau\tau$  process will be the main channel of interest in early data, despite having a cross-section approximately an order of magnitude less than  $W \rightarrow \tau\nu$ . The presence of an additional  $\tau$  lepton can be used to further suppress backgrounds. Studies involving this process usually consider the case when one  $\tau$  lepton decays hadronically and the other leptonically ( $\tau_{\text{lep}}$ ). This also allows the events to be selected using an electron or muon trigger, leading to an unbiased sample of  $\tau_{\text{had}}$  candidates.

Backgrounds to  $Z \rightarrow \tau\tau$  include dijet production,  $W \rightarrow l\nu$  ( $l = e, \mu, \tau$ ),  $Z \rightarrow ee$ , and  $t\bar{t}$  events. Events are selected by requiring an isolated electron or muon with  $p_T > 15$

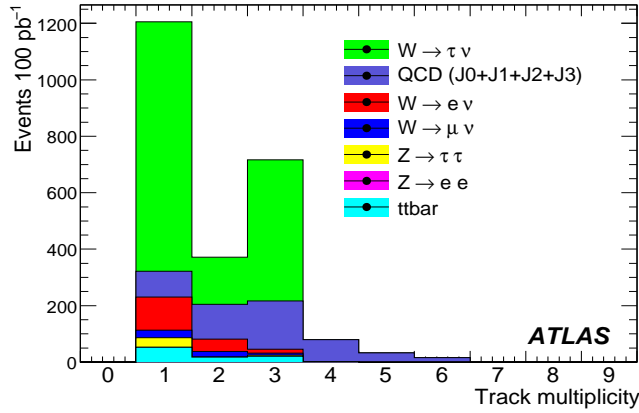


**FIGURE 2.** The track multiplicity spectrum for  $\tau_{\text{had}}$  candidates in  $100 \text{ pb}^{-1}$  for  $W \rightarrow \tau \nu$  and background processes.

GeV, an identified  $\tau_{\text{had}}$  lepton with  $p_{\text{T}} > 15 \text{ GeV}$ ,  $E_{\text{T}}^{\text{miss}} > 20 \text{ GeV}$ , transverse mass of the lepton and  $E_{\text{T}}^{\text{miss}}$  satisfying  $M_{\text{T}}(\text{lep}, E_{\text{T}}^{\text{miss}}) < 30 \text{ GeV}$ , sum of calorimeter energy deposits  $\Sigma E_{\text{T}}^{\text{calo}} < 400 \text{ GeV}$ , and a veto on  $b$ -jets. The lepton and  $\tau_{\text{had}}$  candidate must also be of opposite sign, with requirements placed on  $\Delta\phi(\text{lep}, \tau_{\text{had}})$  to ensure that they are not back-to-back.

With  $100 \text{ pb}^{-1}$ , 520 events are expected with a visible mass  $37 < M_{\text{vis}}(\text{lep}, \tau_{\text{had}}) < 75 \text{ GeV}$  with a signal to background ratio of 5:1. The distribution of  $M_{\text{vis}}(\text{lep}, \tau_{\text{had}})$  is shown in Fig. 3 (left). Backgrounds from dijet and  $W$  production for this channel can be evaluated using data driven techniques, using control samples of same sign events, and the high  $M_{\text{T}}(\text{lep}, E_{\text{T}}^{\text{miss}})$  region.

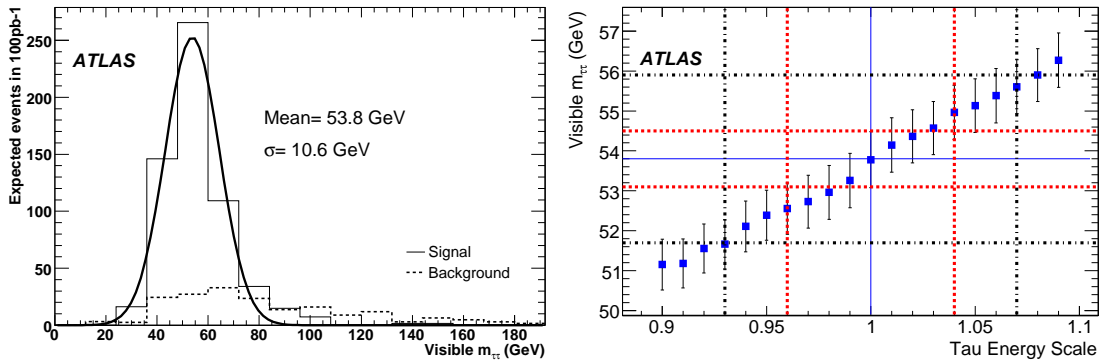


**FIGURE 3.** Left: The visible mass  $M_{\text{vis}}(\text{lep}, \tau_{\text{had}})$  distribution for  $Z \rightarrow \tau \tau$  events and backgrounds in  $100 \text{ pb}^{-1}$  of data. Right: The reconstructed visible mass  $M_{\text{vis}}(\text{lep}, \tau_{\text{had}})$  as a function of the  $\tau_{\text{had}}$  energy scale (uncertainties shown are statistical only).

Since this channel provides an unbiased sample of  $\tau_{\text{had}}$  candidates, tag and probe methods can be used to measure the identification efficiency for both the offline reconstruction and trigger. In addition, the visible mass distribution can be used to evaluate the  $\tau_{\text{had}}$  lepton energy scale, shown in Fig. 3 (right).

## Searches for new phenomena with $\tau$ final states

Many models that describe phenomena beyond the Standard Model predict signatures that are observable at the LHC with  $\tau$  leptons in the final state. For instance, some SUSY models predict an excess of events with  $\tau$  leptons, particularly if the parameter  $\tan\beta$  is large [6], when the  $\tilde{\tau}$  is predicted to be the next-to-lightest SUSY particle.

Strategies for SUSY searches with  $\tau$  lepton final states have been evaluated assuming  $1 \text{ fb}^{-1}$  of data, requiring a jet with  $p_T > 100 \text{ GeV}$ , three other jets with  $p_T > 50 \text{ GeV}$ , a  $\tau_{\text{had}}$  candidate with  $p_T > 40 \text{ GeV}$ ,  $E_T^{\text{miss}} > 100 \text{ GeV}$ , and a veto on isolated electrons or muons. The  $E_T^{\text{miss}}$  is separated from the jets by requiring  $\Delta R(E_T^{\text{miss}}, \text{jet}) > 0.2$  and also must satisfy  $E_T^{\text{miss}} > 0.2 \times M_{\text{eff}}$  where the effective mass  $M_{\text{eff}}$  is the scalar sum of the  $p_T$  of the jets, the  $E_T^{\text{miss}}$  and  $p_T^{\tau_{\text{had}}}$ . Additionally, the transverse sphericity greater than 0.2 is required, and a requirement of  $M_T(E_T^{\text{miss}}, \tau_{\text{had}}) > 100 \text{ GeV}$  is also imposed.

The main backgrounds for this channel include  $t\bar{t}$ ,  $W + \text{jets}$ , and  $Z + \text{jets}$  processes. The discovery reach for this event selection in the mSUGRA  $m_0 - m_{1/2}$  plane with  $\tan\beta = 50$  is shown in Fig. 4 for  $1 \text{ fb}^{-1}$  of integrated luminosity. The sensitivity of this search is comparable to similar search strategies without  $\tau_{\text{had}}$  lepton selection.

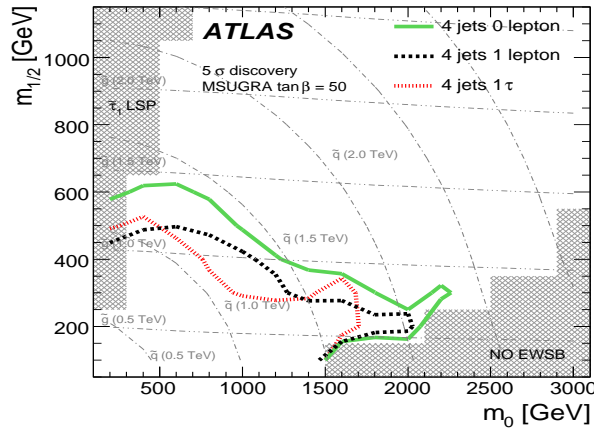


**FIGURE 4.** The  $5\sigma$  discovery contours in the mSUGRA  $m_0 - m_{1/2}$  plane with  $\tan\beta = 50$  for  $1 \text{ fb}^{-1}$ . The 4 jets + 1  $\tau_{\text{had}}$  has similar sensitivity to the 4 jets search and the 4 jet + 1 lepton search.

Other models posit the existence of heavier gauge bosons [7] such as the  $Z'$  boson, with some predicting enhanced couplings to  $\tau$  leptons. The most promising prospects occur in the  $Z' \rightarrow \tau_{\text{had}} \tau_{\text{lep}}$  channel. In this case, an isolated electron (muon) with  $p_T > 27(22) \text{ GeV}$ , an identified  $\tau_{\text{had}}$  lepton with  $p_T > 60 \text{ GeV}$  and opposite charge,  $E_T^{\text{miss}} > 30 \text{ GeV}$  and  $M_T(\text{lep}, E_T^{\text{miss}}) < 35 \text{ GeV}$  are required. The vector sum of  $E_T^{\text{miss}}$ ,  $p_T^{\tau_{\text{had}}}$  and  $p_T^{\text{lep}}$  must be less than  $70 \text{ GeV}$ , and a visible mass cut of  $M_{\text{vis}}(\text{lep}, \tau_{\text{had}}) > 300 \text{ GeV}$  is applied. To extract the invariant mass of the  $\tau\tau$  system, the collinear approximation is used, which infers the direction of neutrinos from  $\tau$  decay by projecting the components of the  $E_T^{\text{miss}}$  on the axes defined by the visible  $\tau$  lepton decay products. A cut on  $\cos\Delta\phi(\text{lep}, \tau_{\text{had}}) > -0.99$  ensures that the lepton and  $\tau_{\text{had}}$  candidates are not back-to-back so that the collinear approximation can be applied.

The distributions for the visible mass  $M_{\text{vis}}(\text{lep}, \tau_{\text{had}})$  and invariant mass  $M_{\text{inv}}(\text{lep}, \tau_{\text{had}})$  attained through the collinear approximation are shown in Fig. 5, where Standard Model couplings for the  $Z$  boson are extended to the  $Z'$  boson, and the mass  $m_{Z'} = 600$  GeV is assumed. A clear excess of  $Z'$  events can be seen over Standard Model backgrounds. Systematic uncertainties are dominated by uncertainties in the integrated luminosity acquired and the  $\tau_{\text{had}}$  lepton energy scale.

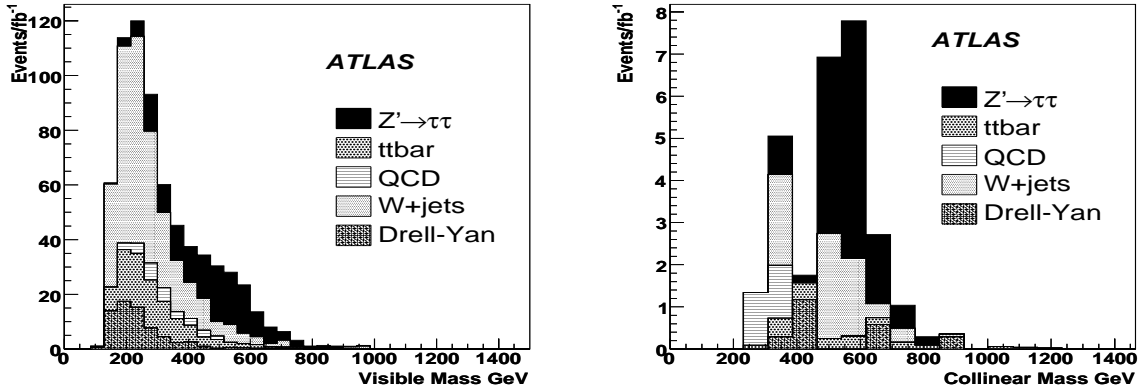


**FIGURE 5.** Left: The visible mass  $M_{\text{vis}}(\text{lep}, \tau_{\text{had}})$  distribution for  $Z'$  events and associated backgrounds ( $m_{Z'} = 600$  GeV). Right: The invariant mass  $M_{\text{inv}}(\text{lep}, \tau_{\text{had}})$  distribution attained from the collinear approximation for  $Z'$  events and associated backgrounds ( $m_{Z'} = 600$  GeV).

## Conclusions

The ATLAS experiment has developed a reconstruction algorithm for hadronically decaying  $\tau$  leptons that exploits their well known properties to suppress fake  $\tau_{\text{had}}$  candidates coming from hadronic jets, electrons or muons. Standard Model processes like  $W$  and  $Z$  boson production will be an abundant source of  $\tau$  leptons, enabling early data measurements of  $\tau_{\text{had}}$  lepton identification,  $\tau_{\text{had}}$  energy scale, and cross-section measurements of  $W$  and  $Z$  boson production in  $\tau$  lepton channels. Once  $\tau_{\text{had}}$  lepton reconstruction is well understood in data, promising searches for new phenomena beyond the Standard Model with  $\tau$  lepton final states can be performed.

## REFERENCES

1. C. Amsler *et al.* (Particle Data Group), *Physics Letters B* 667, 1 (2008).
2. The ATLAS Collaboration, G. Aad *et al.*, “Expected Performance of the ATLAS Experiment, Detector, Trigger, and Physics”, CERN-OPEN-2008-020, Geneva, (2008).
3. The ATLAS Collaboration, G. Aad *et al.*, “The ATLAS Experiment at the CERN Large Hadron Collider”, *JINST* 3 (2008) S08003.
4. S.D. Ellis *et al.*, “Jets in hadron-hadron collisions”, *Prog.Part.Nucl.Phys.* 60:484-551, (2008).
5. C. Schwanenberger (for the H1 Collaboration), “The Jet Calibration in the H1 Liquid Argon Calorimeter”, arXiv:physics/0209026v1 [physics.ins-det] (2002).
6. S.P. Martin, “A Supersymmetry Primer”, arXiv:hep-ph/9709356v5, (1997).
7. H. Georgi, S. Weinberg, “Neutral currents in expanded gauge theories”, *Phys. Rev. D*, **17**, 275, (1978).